journal

J. Am. Ceram. Soc., 89 [1] 236–240 (2006)
DOI: 10.1111/j.1551-2916.2005.00668.x

Properties of Tm^{3+}-Doped Germanotellurite Glasses for S-Band Amplifier

Yuki Kishi and Setsuhisa Tanabe*,†

Graduate School of Human and Environmental Studies, Kyoto University, Sakyo-ku, Kyoto 606-8501, Japan

Optical and material properties of $(75-x)TeO_2$–$xGeO_2$–$20ZnO$–$5Na_2O$–$0.1Tm_2O_3$ glasses were investigated as candidate materials for an S-band Tm-doped fiber amplifier (TDFA). With increasing GeO_2 content, the lifetime and the quantum efficiency of the 1.46 μm emission decreased slightly, while the emission bandwidth, the Vickers hardness, and thermal stability of the glass improved monotonically. Above 20 mol% GeO_2, the quantum efficiency decreased more rapidly with increasing GeO_2. We conclude that addition of a small amount of germania may improve material properties without deteriorating the optical properties of doped Tm^{3+}, and thus the germanotellurite fiber may be a more reliable material for the S-band TDFA in wavelength-division-multiplexing telecommunication.

I. Introduction

In the wavelength-division-multiplexing (WDM) network system, there is an emergent demand for optical amplifiers, which can be used in the wavelength range between 1.46 and 1.65 μm, in addition to the C-band (1.53 ~ 1.56 μm) covered with the present silica-based Er-doped fiber amplifiers (EDFA). Tellurite-based EDFA, which also shows material properties better than those of fluorides, was reported to have an 80-nm-wide gain up to 1.61 μm (L-band).[1] In order to extend the telecommunication band, the fluoride-based Tm-doped fiber amplifier (TDFA) can be used for the 1.45–1.49 μm band (S^+-band).[2] The fluoride-based TDFA has a quantum efficiency high enough to amplify the optical signal in the S^+-band because of its lower phonon energy. However, it still presents difficulties compared with the use of EDFA. One of the reasons for the inferior performance of TDFA is the longer lifetime of the terminal $^3F_4$ level than that of the initial $^3H_4$ level.[3] The performance of the TDFA is improved using an upconversion pumping scheme with a 1.06 μm laser, which produces a population inversion. Codoping of other lanthanide ions, such as Ho^{3+}, was also found to improve the population inversion by means of an energy transfer from the $^3F_4$ level.[4,5] Another disadvantage of TDFA is that the chemical durability and the mechanical properties of the fluoride glasses are inferior to the oxide glasses as an optical fiber used in the long term. Oxide glasses such as tellurite are known as a good matrix for doping rare-earth ions because of their lower phonon energy compared with other oxide glasses. Tellurite-based TDFA has good 1.46 μm emission properties of Tm^{3+}, but the thermal stability and the chemical durability of this glass matrix are lower than those of other oxide glasses.[6] In this study, in order to seek the possibility to compensate for these disadvantages of the tellurite glass, GeO_2 was added to the glass composition.[7] The compositional dependence of the emission properties of Tm^{3+} and the mechanical and thermal properties of matrix glasses were investigated.

II. Experimental Procedure

(1) Glass Preparation and Optical Measurement

Germanotellurite glasses with compositions of $(75-x)TeO_2$–$xGeO_2$–$20ZnO$–$5Na_2O$–$0.1Tm_2O_3$ ($x = 0$–75) were prepared. Each batch (10 g) was well mixed. Some batches with a lower GeO_2 content ($x = 0$–20) were melted in a gold crucible at 850°C, and other batches with a higher GeO_2 content ($x = 30$–75) were melted in a platinum crucible for 1 h at 900°–1300°C depending on the glass composition. The melt was poured into a stainless-steel mold, which was preheated around the glass transition temperature (T_g), and annealed at around T_g for 1 h. The glass was cut and polished for optical measurements. The density of the obtained glasses was measured by the Archimedes method using kerosene as an immersion liquid.

Thermal analysis was carried out using a differential thermal analyzer (Rigaku, Thermal plus, TG-DTA TG8120, Akishima, Japan) at a heating rate of 10°C/min from room temperature to 500°C ($x = 0$–20) and to 1000°C ($x = 30$–75).

Absorption spectra were measured at room temperature with a scanning spectrophotometer (Shimadzu, UV-3101PC, Kyoto, Japan) in the range of 400–2000 nm. 1 mol% Tm_2O_3-doped glasses were prepared to obtain a large absorption cross-section, since the glass samples doped with 0.1 mol% Tm_2O_3 showed too small an absorption cross-section to carry out the Judd–Ofelt (J–O) analysis precisely.

Refractive indices of all samples at 633, 1304, and 1550 nm were measured by the prism-coupling method. The wavelength dependence of the refractive indices, n, of all samples was obtained by,

$$n(\lambda) = A + \frac{B}{\lambda^2} + \frac{C}{\lambda^4} \quad (1)$$

where λ is the wavelength, and A, B, and C are coefficients obtained by least-square fitting with the measured refractive indices.

Fluorescence spectra in the range of 1200–2200 nm were measured by using a 792 nm laser diode (Sony, SLD-304XT, Tokyo, Japan), a monochromator (Nikon, G-250, Tokyo, Japan), and a PbS photo-detector (Hamamatsu Photonics, P4638, Hamamatsu, Japan). For the fluorescence lifetime measurement, the luminescence decay curves were recorded with a digital storage oscilloscope (LeCroy, LS-140, 100 MHz, Chestnut Ridge, NY) to calculate the lifetime by least-squares fitting. An InGaAs photodiode (Electro-Optical Systems Inc., IGA-010-H, Phoenixville, PA) was used to detect the lifetime of the $^3H_4$ level (1.46 μm), and another InGaAs photodiode (Electro-Optical Systems Inc., IGA-2.2-010-TE2-H) was used to detect the lifetime of the $^3F_4$ level (1.8 μm).

The Vickers hardness of the glass was measured by loading 50 g for 15 s, using a Vickers hardness tester (Matsuzawa, MXT-α, Osaka, Japan).

J. Ballato—contributing editor

Manuscript No. 20228. Received February 28, 2005; approved June 29, 2005.
Supported by the Grants-in-Aid for Scientific Research on Priority Area (Rare Earth Materials; No.16080209) from the Ministry of Education, Science and Culture, Japan.
*Member, American Ceramic Society.
†Author to whom correspondence should be addressed. e-mail: stanabe@gls.mbox.media.kyoto-u.ac.jp

(2) J–O Analysis

The J–O theory[8,9] is the most useful theory in estimating the probability of the forced electric dipole transitions of rare-earth ions in various environments.[10,11] It is also usually used to study the local ligand field (asymmetry, bond covalency) of rare-earth ions from the three Ω_t ($t = 2,4,6$) parameters.[12,13] According to the J–O theory, the line strength for the electric dipole transition between an initial J manifold $|(S, L)J\rangle$ and a final J' manifold $|(S', L')J'\rangle$ is obtained by

$$S^{ed}[(S,L)J;(S',L')J'] = \sum_{t=2,4,6} \Omega_t \left| \left\langle (S,L)J \| U^{(t)} \| (S',L')J' \right\rangle \right|^2 \quad (2)$$

where the three terms $\langle \| U^{(t)} \| \rangle$ are the reduced matrix elements of the unit tensor operators calculated in the intermediate-coupling approximation, and the parameters Ω_2, Ω_4, and Ω_6 are the intensity parameters, which contain the effects of the crystal-field terms, radial integrals of an electron, and so on. Since the reduced matrix elements $\langle \| U^{(t)} \| \rangle$ are characteristics constant in each transition, the three Ω_t ($t = 2,4,6$) parameters can be obtained experimentally from the line strengths of at least three absorption bands using a least-squares fitting. In this study, four absorption bands of $^3F_4$, $^3H_4$, $^3F_{2,3}$, and $^1G_4$ were used. The $^3H_5 \leftarrow {}^3H_6$ band at 1.2 μm was not used, because this transition includes the magnetic-dipole contribution. To calculate the S^{ed} for each band from the integrated area of the absorption cross section, the refractive index value at each wavelength was calculated using the values of A, B, and C in Eq. (1).

III. Results

(1) 1.46 μm Emission Spectra and Absorption Spectra

Figure 1 shows the fluorescence spectra of $(75-x)TeO_2$–$xGeO_2$–$20ZnO$–$5Na_2O$–$0.1Tm_2O_3$ glasses. A 1.46 μm emission band due to the transition from the $^3H_4$ level to the $^3F_4$ level (Fig. 2) and a 1.8 μm emission band due to that from the $^3F_4$ level to the $^3H_6$ level were observed. The spectra are normalized at 1.8 μm emission band for intensity comparison of 1.46 μm emission. The relative intensity of the 1.46 μm emission decreased with increasing GeO_2 content. Figure 3 shows the compositional dependence of the ratio of integrated intensity of the 1.46–1.8 μm emission band. The integration was carried out after converting the abscissa into wavenumber scale. The ratio decreased with increasing GeO_2 content.

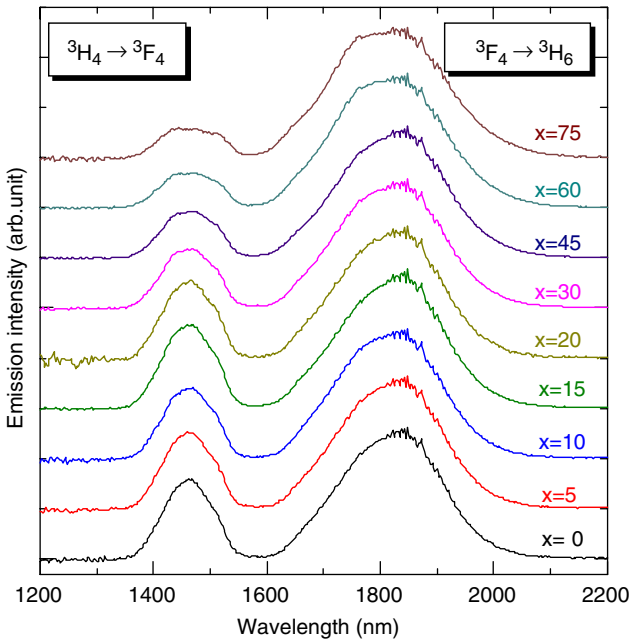

Fig. 1. Fluorescence spectra of $(75-x)TeO_2$–$xGeO_2$–$20ZnO$–$5Na_2O$–$0.1Tm_2O_3$ glasses.

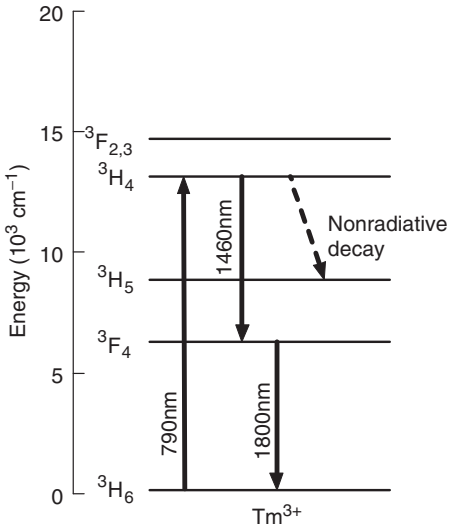

Fig. 2. Energy level diagram of Tm^{3+} ion.

Figure 4 shows the absorption spectra of $(75-x)TeO_2$–$xGeO_2$–$20ZnO$–$5Na_2O$–$0.1Tm_2O_3$ glasses. Five absorption bands from the ground state $^3H_6$ level to the $^1G_4$, $^3F_{2,3}$, $^3H_4$, $^3H_5$, and $^3F_4$ levels were observed in the range of 400–2000 nm.

(2) Fluorescence Lifetimes of the $^3H_4$ and $^3F_4$ Levels of Tm^{3+}

Figure 5 shows the compositional dependence of the fluorescence lifetime of the $^3H_4$ and $^3F_4$ levels in $(75-x)TeO_2$–$xGeO_2$–$20ZnO$–$5Na_2O$–$0.1Tm_2O_3$ glasses. The lifetime of the $^3F_4$ level increased with increasing GeO_2 content. On the other hand, the lifetime of the $^3H_4$ level gradually decreased in the range of lower GeO_2 content and rapidly decreased in the range of higher GeO_2 content ($x > 30$).

(3) Thermal Stability and Vickers Hardness of Germanotellurite Glasses

Figure 6 shows the compositional dependence of glass transition temperature, T_g, the onset of crystallization temperature,

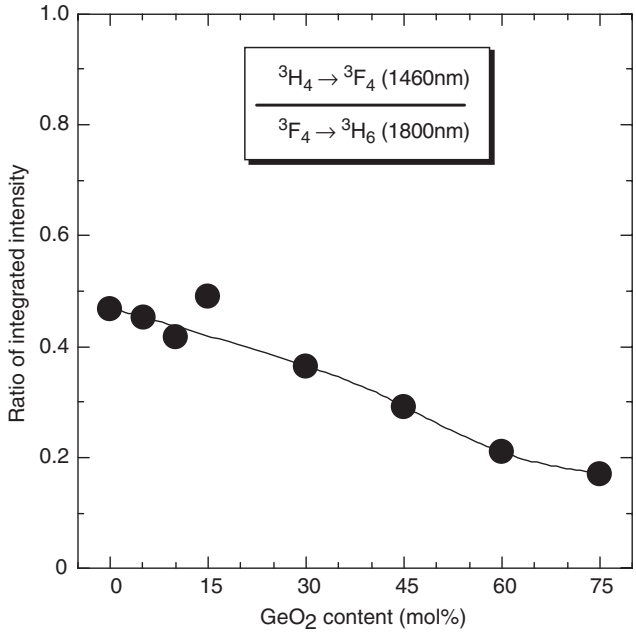

Fig. 3. Ratio of integrated intensity of the 1.46–1.8 μm emission band.

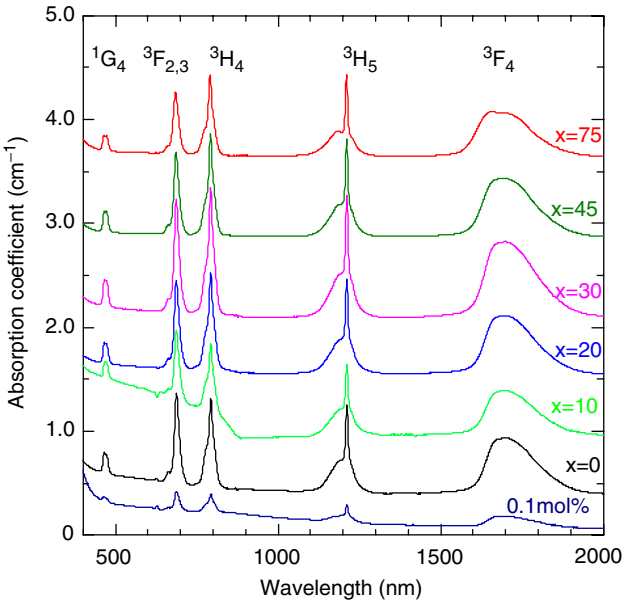

Fig. 4. Absorption spectra of $(75-x)TeO_2$–$xGeO_2$–20ZnO–$5Na_2O$–$0.1Tm_2O_3$ glasses.

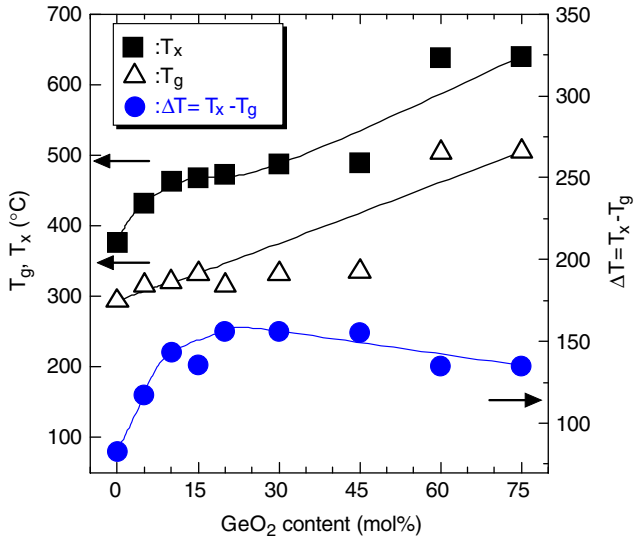

Fig. 6. Glass transition temperature, T_g, onset of crystallization temperature, T_x, and their difference, ΔT ($=T_x-T_g$), of $(75-x)TeO_2$–$xGeO_2$–20ZnO–$5Na_2O$–$0.1Tm_2O_3$ glasses.

T_x, and their difference, ΔT ($=T_x-T_g$), which is used as a rough measure of thermal stability. Both T_g and T_x increased with increasing GeO_2 content. The thermal stability parameter ΔT rapidly increased in the range of GeO_2 content less than 20 mol%, and gradually decreased in the range of over 30 mol% GeO_2.

Figure 7 shows the compositional dependence of the Vickers hardness of $(75-x)TeO_2$–$xGeO_2$–20ZnO–$5Na_2O$–$0.1Tm_2O_3$ glasses. It increased monotonically with increasing GeO_2 content.

IV. Discussion

(1) Compositional Dependence of the Quantum Efficiency

In order to incorporate good gain performance into an amplifier material, evaluation of the quantum efficiency of the initial level of the amplification transition is important. Generally, the quantum efficiency of the emission is given by

$$\eta = \tau_f \times A \tag{3}$$

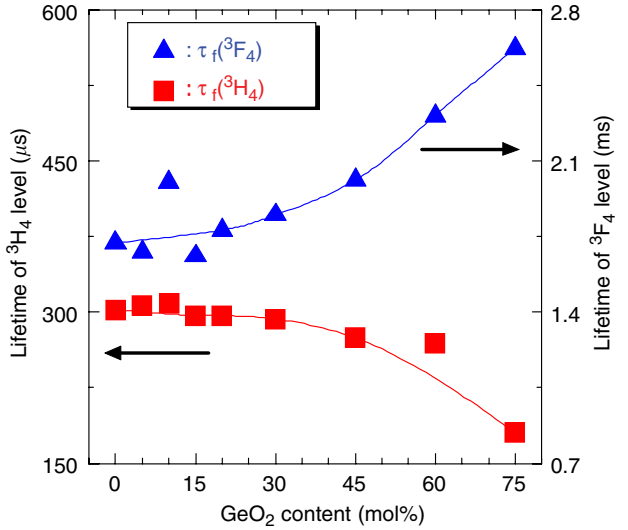

Fig. 5. Fluorescence lifetime of the $^3H_4$ and $^3F_4$ level of Tm^{3+} in $(75-x)TeO_2$–$xGeO_2$–20ZnO–$5Na_2O$–$0.1Tm_2O_3$ glasses.

where τ_f is the fluorescence lifetime and A is the spontaneous emission rate. The fluorescence lifetime τ_f can be given by

$$\tau_f^{-1} = A + W_{NR} \tag{4}$$

where W_{NR} is the non-radiative decay rate. The spontaneous emission rate A of the 4f electric-dipole transitions can usually be obtained with the three J–O parameters. From the obtained absorption spectra shown in Fig. 4, the J–O analysis was carried out.

Figure 8 shows the compositional dependence of the J–O parameter of Tm^{3+} in $(75-x)TeO_2$–$xGeO_2$–20ZnO–$5Na_2O$–$0.1Tm_2O_3$ glasses ($x=0$–75). These J–O parameters Ω_t ($t=2,4,6$) were calculated for each sample by using four absorption bands at the respective energy levels of $^1G_4$, $^3F_{2,3}$, $^3H_4$, and $^3F_4$. It can be seen that the Ω_2 parameter reached a maximum at about $x=30$ mol%.

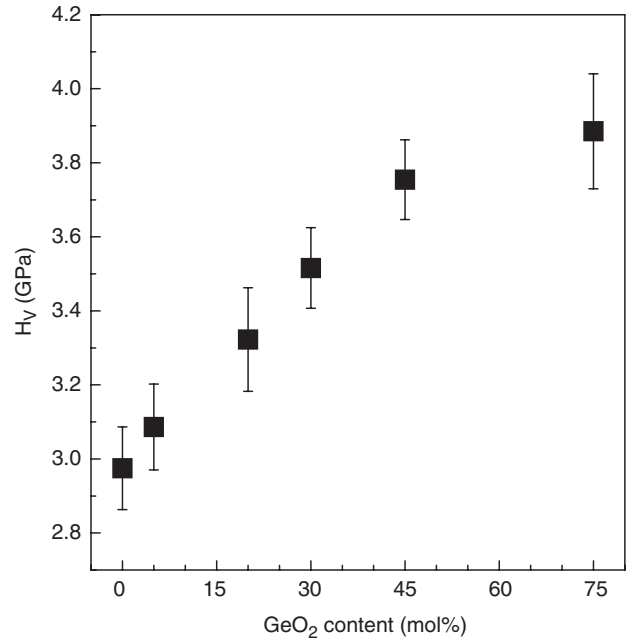

Fig. 7. Vickers hardness of $(75-x)TeO_2$–$xGeO_2$–20ZnO–$5Na_2O$–$0.1Tm_2O_3$ glasses.

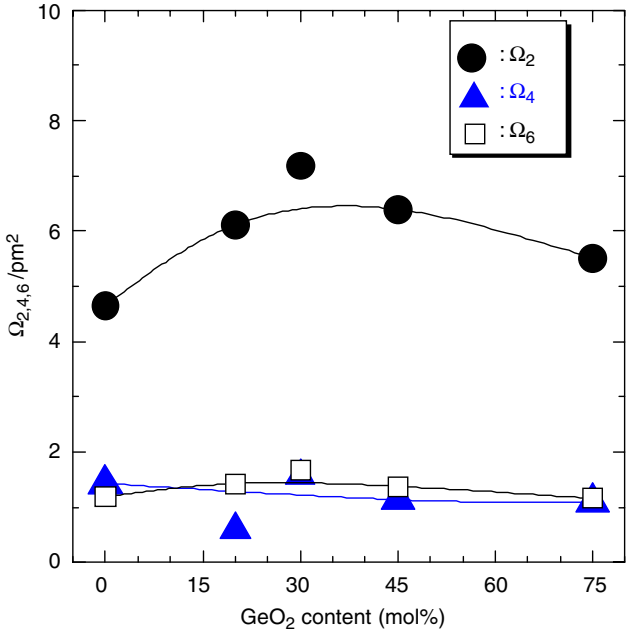

Fig. 8. Judd–Ofelt parameters of Tm^{3+} in $(75-x)TeO_2$–$xGeO_2$–$20ZnO$–$5Na_2O$–$0.1Tm_2O_3$ glasses.

The spontaneous emission rate A from an energy level to lower energy levels was calculated by

$$A = \frac{64\pi^4 e^2}{3h(2J'+1)} \times \frac{1}{\lambda^3} \times \frac{n(n^2+2)^2}{9} S_{JJ'} \tag{5}$$

where n is the refractive index and $S_{JJ'}$ is the line strength calculated with the obtained J–O parameters and corresponding $<U^{(t)}>2$'s in Eq. (2). Figure 9 shows the spontaneous emission rate A from the $^3H_4$ level to lower energy levels and that from the $^3F_4$ level to the $^3H_6$ level of Tm^{3+}. The A from the $^3H_4$ level to the lower energy levels was around 3000 s^{-1} in the range of GeO_2 content less than 20 mol%, and decreased at a range over 20 mol% GeO_2 content. Also, that from the $^3F_4$ level to the $^3H_6$ level slightly decreased.

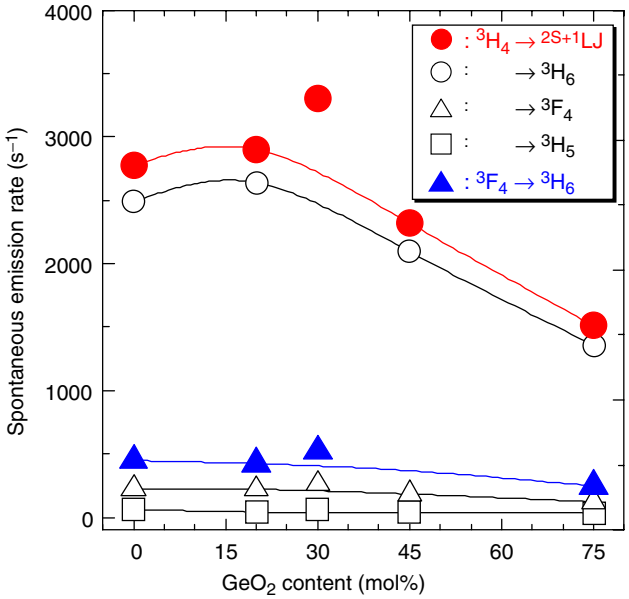

Fig. 9. Spontaneous emission rate A from the $^3H_4$ and $^3F_4$ levels to lower energy levels of Tm^{3+} in $(75-x)TeO_2$–$xGeO_2$–$20ZnO$–$5Na_2O$–$0.1Tm_2O_3$ glasses.

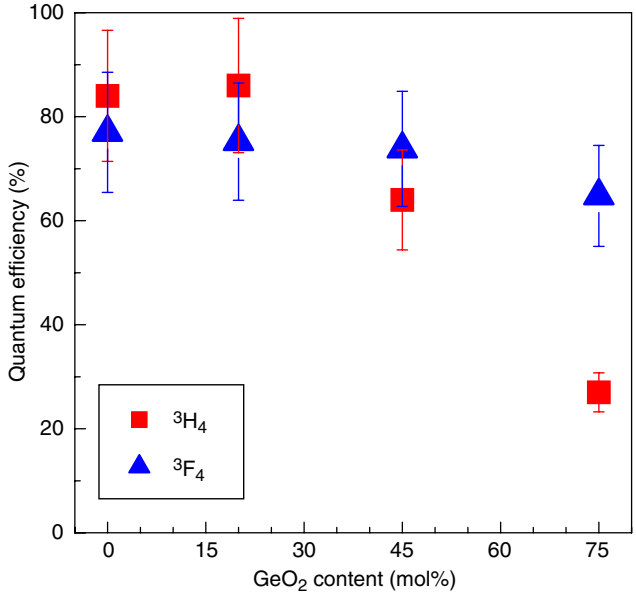

Fig. 10. Quantum efficiency of the $^3H_4$ and the $^3F_4$ levels of Tm^{3+}.

From Eq. (3), the quantum efficiencies, η, of the Tm^{3+} emissions in the glasses were calculated. Figure 10 shows the compositional dependence of the quantum efficiency of the $^3H_4$ and the $^3F_4$ levels of Tm^{3+} in $(75-x)TeO_2$–$xGeO_2$–$20ZnO$–$5Na_2O$–$0.1Tm_2O_3$ glasses. It can be seen that the quantum efficiency of the $^3H_4$ level remained about 80% in the range of GeO_2 content less than 30 mol% and rapidly decreased at over 30 mol% GeO_2 content range. The quantum efficiency from the $^3F_4$ level slightly decreased between 80 and 70% with increasing GeO_2 content. Therefore, the monotonic increase of the $^3F_4$ lifetime with GeO_2 content can be ascribed mostly to the contribution of decreasing A. On the other hand, a non-radiative decay rate contributes to the decreasing tendency of η and τ_f of the $^3H_4$ level.

(2) Influence of GeO_2 Content on 1.46 μm Emission Intensity

As shown in Figs. 1 and 3, the emission intensity of the 1.46 μm band decreased with increasing GeO_2 content. This is caused by the increasing non-radiative decay rate W_{NR} from the $^3H_4$ level to the $^3H_5$ level of the Tm^{3+}. From Fig. 5 and Eq. (4), it is suggested that W_{NR} from the $^3H_4$ level is increased, since the spontaneous emission rate A from the $^3H_4$ level to lower energy levels decreased as shown in Fig. 9. The non-radiative decay rate W_{NR} is expressed by

$$W_{NR} = W_p + W_{ET} \tag{6}$$

where W_p is the multiphonon decay rate and W_{ET} is the relaxation by energy transfer. The contribution of W_{ET} can be ignored in this situation, because the Tm concentration is low enough and almost constant against GeO_2 content. Thus, the factor dominating the quantum efficiency is W_p, which is associated with the phonon energy. W_p is expressed by[14]

$$W_p = W_0 \exp\left(\frac{-\alpha\Delta E}{\hbar\omega}\right) \tag{7}$$

where ΔE is the energy gap to the next lower level and $\hbar\omega$ is the phonon energy of the matrix glass. According to Eq. (7), W_{NR} should be much larger in silicate glass with a higher phonon energy ($\hbar\omega = 1100\ cm^{-1}$) than tellurite glass ($\hbar\omega = 750\ cm^{-1}$). It is known that the phonon energy of Te–O is 750 cm^{-1} and that of Ge–O is around 850 cm^{-1}. This difference in phonon energy can cause a change of W_p from the tellurite host and the germanate host. Addition of GeO_2 to TeO_2 glasses can increase the

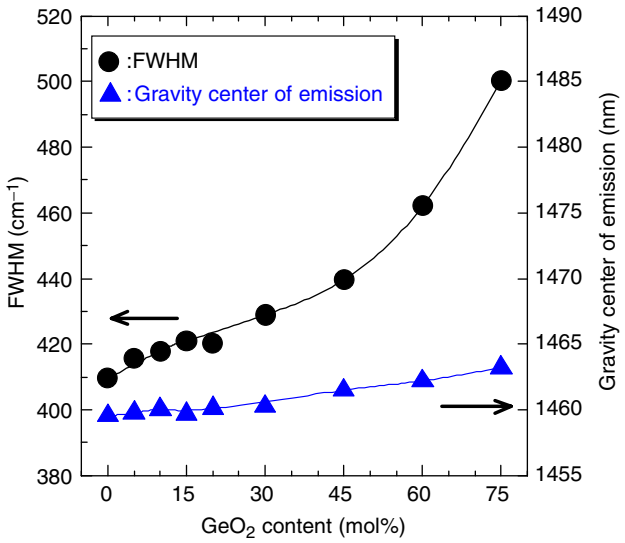

Fig. 11. Bandwidth and the gravity center of the 1.46 μm emission band in $(75-x)TeO_2$–$xGeO_2$–20ZnO–5Na_2O–0.1Tm_2O_3 glasses.

average phonon energy of the matrix glass, resulting in an increase of W_{NR}. As shown in the Tm^{3+} energy diagram (Fig. 2), there is a $^3H_5$ level between the $^3H_4$ and $^3F_4$ levels. The energy gap ΔE between the $^3H_4$ and $^3H_5$ levels is about 4300 cm^{-1}. It can be said that the quantum efficiency of the $^3H_4$ level decreased with increasing W_{NR} at a higher GeO_2 content.

As a result, the 1.46 μm emission intensity of Tm^{3+} decreased with increasing GeO_2 content. Because the signal gain performance by the induced emission in the fiber amplifier is directly related to the quantum efficiency of the initial level, the small quantum efficiency and emission intensity could be disadvantageous for a 1.46 μm amplifier.

The non-radiative decay, W_{NR}, from the $^3F_4$ level can be negligibly small in hosts with moderate phonon energy,[15] since no energy levels exist between the $^3F_4$ and the $^3H_6$ levels, and this energy gap is about 5500 cm^{-1}, which is large enough for host glasses with a phonon energy lower than silicate ($\hbar\omega = 1100$ cm^{-1}). Therefore, the increasing lifetime of the $^3F_4$ level can be ascribed mostly to the decreasing spontaneous emission rate A from the $^3F_4$ level. This fact is also evidence of large η of the $^3F_4$ level in these glasses. Therefore, the relative intensity of 1.46/1.8 μm bands can be a measure of η of the $^3H_4$ level.[16]

(3) Influence of GeO_2 Content on the S-Band Emission Bandwidth

In the WDM telecommunication system, amplifiers with a broader gain spectrum are required. Also, an amplifier in the S-band region (1.49–1.52 μm) would be important, because there exists a wavelength gap between the C-band and S^+-band, which are covered with the EDFA and fluoride TDFA, respectively. One of the methods of covering this "S-band gap" is the gain-shifted TDFA by a dual-wavelength pumping scheme.[17] Since this scheme requires a slightly complicated coupler configuration, it would be ideal to develop a material that originally has an emission band in the S-band. Figure 11 shows the bandwidth and the gravity center of the $^3H_4 \rightarrow {}^3F_4$ emission band in $(75-x)TeO_2$–$xGeO_2$–20ZnO–5Na_2O–0.1Tm_2O_3 glasses. With increasing GeO_2 content, the bandwidth represented as full-width at half-maximum (FWHM) increased from 410 to 500 cm^{-1} and the gravity center of emission slightly shifted to the longer wavelength side. These spectral changes are possibly due to the variation of the ligand fields around the Tm^{3+} ion and coordination of a higher number of Ge–O bonds. Thus, glasses with a higher GeO_2 content can be used as a host material for TDFA at a longer wavelength range of S-band, if η of the $^3H_4$ level is high enough.

In terms of material properties such as fiberizability and mechanical strength, addition of GeO_2 to the tellurite glass has a good influence as indicated in the increasing tendencies of ΔT and H_v in Figs. 6 and 7, respectively.

V. Conclusion

Tm-doped germanotellurite glasses were prepared for the matrix glass of the S-band amplifier in WDM telecommunication. The compositional dependence of the optical properties such as emission, lifetime, and quantum efficiency, and the mechanical properties such as thermal stability and Vickers hardness were investigated. The quantum efficiency of the $^3H_4$ level of Tm^{3+} was less than 80% in the range of GeO_2 content more than 30 mol%; hence, the 1.46 μm emission efficiency decreased. However, the 1.46 μm emission band broadened toward the long wavelength region. The thermal stability and Vickers hardness of the matrix glasses had improved. Germanotellurite glass containing 20–30 mol% GeO_2 may be desirable for the host material of TDFAs.

Acknowledgments

The authors would like to thank Prof. H. Kozuka and Mr. K. Ishida of Kansai University for their help with the Vickers hardness measurement. They also thank Mr. H. Hayashi and Dr. N. Sugimoto of Asahi Glass Company for the refractive index measurement.

References

[1]A. Mori, Y. Ohishi, and S. Sudo, "Erbium-Doped Tellurite Glass Fibre Laser and Amplifier," *Electron. Lett.*, **33** [10] 863–4 (1977).
[2]T. Sakamoto, A. Aozasa, T. Kanamori, K. Hoshino, M. Yamada, and M. Shimizu. "Gain-Equalized Thulium-Doped Fiber Amplifiers for 1460 nm-Band WDM Signals"; pp. 50–3 in *1999 Technical Digest of the 10th Optical Amplifiers and their Applications*, WD2-1 (OSA, Washington, DC, June, 1999).
[3]R. M. Percival, D. Szebesta, and J. R. Williams, "Highly Efficient 1.064 μm Upconversion Pumped 1.47 μm Thulium Doped Fluoride Fiber Laser," *Electron. Lett.*, **30** [13] 1057–8 (1994).
[4]T. Sakamoto, M. Shimizu, T. Kanamori, Y. Terumuma, Y. Ohishi, M. Yamada, and S. Sudo, "1.4 μm-Band Gain Characteristics of a Tm–Ho-Doped ZBLYAN Fiber Amplifier Pumped in the 0.8 μm-Band," *IEEE Photonics Tech. Lett.*, **7** [9] 983–5 (1995).
[5]S. Tanabe "Optical Properties of Tm-Doped Tellurite Glasses for 1.4 μm Amplifier"; pp. 85–92 in Proceedings of SPIE, Vol. 4282, *Rare-Earth-Doped Materials and Devices V* (Photonics West, Optoelectronics 2001, San Jose, January), Ed. by S. Jiang, 2001.
[6]J. S. Wang, E. M. Vogel, and E. Shitzer, "Tellurite Glass: A New Candidate for Fiber Devices," *Opt. Mater.*, **3**, 187–203 (1994).
[7]X. Feng, S. Tanabe, and T. Hanada, "Spectroscopic Properties and Thermal Stability of Er^{3+}-Doped Gemanotellurite Glasses for Broadband Fiber Amplifiers," *J. Am. Ceram. Soc.*, **84**, 165–71 (2001).
[8]B. R. Judd, "Optical Absorption Intensities of Rare-Earth Ions," *Phys. Rev.*, **127** [3] 750–61 (1962).
[9]G. S. Ofelt, "Intensities of Crystal Spectra of Rare-Earth Ions," *J. Chem. Phys.*, **37** [3] 511–20 (1962).
[10]W. F. Krupke, "Induced-Emission Cross Section in Neodymium Laser Glass," *IEEE J. Quantum Electron.*, **QE-10** [4] 450–7 (1974).
[11]R. R. Jacobs and M. J. Weber, "Dependence of the $^4F_{3/2} \rightarrow {}^4I_{11/2}$ Induced-Emission Cross Section for Nd^{3+} on Glass Composition," *IEEE J. Quantum Electron.*, **QE-12** [2] 102–11 (1976).
[12]S. Tanabe, T. Ohyage, N. Soga, and T. Hanada, "Compositional Dependence of Judd–Ofelt Parameters of Er^{3+} Ions in Alkali–Metal Borate Glasses," *Phys. Rev. B*, **46** [6] 3305–10 (1992).
[13]S. Tanabe, T. Ohyage, T. Todoroki, T. Hanada, and N. Soga, "Relationship Between the Ω_6 Intensity Parameters of Er^{3+} Ions and the ^{151}Eu Isomer Shift in Oxide Glasses," *J. Appl. Phys.*, **73** [12] 8451–4 (1993).
[14]T. Miyakawa and D. L. Dexter, "Phonon Sidebands, Multiphonon Relaxation of Excited States, and Phonon-Assisted Energy Transfer Between Ions in Solids," *Phys. Rev. B*, **1**, 2961–9 (1970).
[15]S. Tanabe, "Design of Rare Earth Doped Amplifiers for WDM Telecommunication"; pp. 67–82 in *Glass Science and Technology on the Threshold of the 3rd Millennium*, Edited by W. Pannhorst. Deutschen Glastechn.Gesellschaft, Frankfurt, 2001.
[16]T. Tamaoka, S. Tanabe, and T. Hanada, "Concentration Dependence of Emission Properties of Tm^{3+}-Doped Tellurite Glasses in Telecommunication Wavelength Region," *J. Ceram. Soc. Jpn.*, **110** [4] 325–8 (2002).
[17]S. Tanabe and T. Tamaoka, "Gain Characteristics of Tm-Doped Fluoride Fiber Amplifier in S-Band by Dual-Wavelength Pumping," *J. Non-Cryst. Solids*, **326&327**, 283–6 (2003). □